Submitted to the
International Conference on High Energy Physics
16-22 August 2004, Beijing, China

Abstract: 5-0342, 11-0343

Sessions: QCD hard interactions and Heavy quarks

Measurement of open beauty production at HERA using a D^*+ muon tag

ZEUS Collaboration

Abstract

The production of beauty quarks via the $D^*\mu$ decay mode has been measured with the ZEUS detector at HERA using an integrated luminosity of 114 pb^{-1}. The low transverse-momentum thresholds for the muon and D^*-meson allow a measurement of beauty production close to the kinematic limit. The signal was extracted using the charge correlations and angular distributions of the muon with respect to the D^* meson. The previously measured photoproduction cross section is extended into the deep inelastic scattering region and compared to NLO QCD predictions.

1 Introduction

This paper reports a measurement of beauty production via the reaction $ep \to eb\bar{b}X \to eD^*\mu X$ using the ZEUS detector at HERA. This reaction offers the advantage of selecting a data sample enriched in b quarks and with strongly suppressed backgrounds from other processes, which allows low-p_T-threshold cuts to be applied. This analysis therefore complements measurements based on leptons with high transverse momentum [1–4]. The previous result from this channel [5], which was focused on photoproduction (PHP), is complemented by a dedicated analysis of the Deep Inelastic Scattering (DIS) part of the cross section.

2 Principle of the measurement

Of particular interest are events in which the muon and D^* originate from the same parent B meson, e.g. $B^0 \to D^{*-}\mu^+\nu$. These yield unlike-sign D^*-muon pairs produced in the same hemisphere and constrained not to exceed the B-meson mass. Another important contribution arises from charm-pair production, where one charm quark fragments into a D^* and the other decays into a muon. This again yields unlike-sign D^*-muon pairs. However, the D^* and the muon will be produced predominantly in opposite hemispheres. Furthermore, beauty-pair production in which the D^* and muon originate from different beauty quarks can yield both like- and unlike-sign D^*-muon combinations, depending on whether the muon is from the decay of the primary beauty quark, or from a secondary charm quark, and whether $B^0 - \bar{B}^0$ mixing has occured. Beauty production is the only source of genuine like-sign D^*-muon pairs. Background contributions to both like- and unlike-sign combinations include events with either fake D^* mesons, originating from combinatorial background, or fake muons. In this analysis, the signal is extracted from the unlike-sign sample, while the like-sign sample is used as a cross check.

3 Analysis

The data used in this analysis were collected in the ZEUS detector [6] during the years 1996-97 (1998-2000), during which a proton beam of 820 (920) GeV collided with an electron or positron beam of 27.5 GeV. The centre-of-mass energy was $\sqrt{s} = 300$ GeV during the period 1996-97 and $\sqrt{s} = 318$ GeV during 1998-2000. In order to present results from the combined data sets, in this paper the measurements from the 1996-97 run have been corrected to correspond to the higher center-of-mass energy of 318 GeV.

All cross sections are therefore quoted for $\sqrt{s} = 318$ GeV. The combined data sample corresponds to a total integrated luminosity of 114 ± 2 pb^{-1}.

The trigger selection required the presence of either a muon, a D^*, or a DIS electron. Because of this redundancy, the trigger efficiency for beauty events was very high, $94 \pm 3\%$ for the inclusive study, and $98 \pm 2\%$ for the DIS selection.

Muons were identified by requiring the presence of a reconstructed segment in the barrel or rear inner muon chambers [6], matched in space to a corresponding track in the central tracking detector [7]. Cuts on the muon transverse momentum ($p_T^\mu > 1.4$ GeV) and pseudorapidity ($-1.75 < \eta^\mu < 1.3$) were applied, ensuring approximately uniform acceptance in the measured kinematic range.

For the inclusive analysis, D^* mesons were selected via the decay $D^{*+} \to D^0(\to K^-\pi^+)\pi_s^+$ (+c.c.) and constraints on the D^0 mass (1.81 GeV $<$ M(Kπ) $<$ 1.92 GeV) and the D^*-D^0 mass difference (0.1435 GeV $<$ M(K$\pi\pi_{\rm s}$) $-$ M(Kπ) $<$ 0.1475 GeV). The D^* transverse momentum and pseudorapidity ranges were $p_T^{D^*} > 1.9$ GeV and $|\eta^{D^*}| < 1.5$, respectively. Additional cuts on the transverse momenta of the D^* decay products were applied in order to reduce the combinatorial background under the D^* mass peaks. Backgrounds from semileptonic D^0 decays were eliminated by requiring that the muon was not one of the D^* decay products. Finally, the $\mu - D^*$ system was required to carry a significant fraction of the total transverse energy of the event.

For the dedicated DIS analysis, the D^* transverse-momentum cut was lowered to $p_T^{D^*} > 1.5$ GeV, the cuts on the D* decay products were adjusted accordingly, and the cut on the $\mu - D^*$ transverse momentum fraction was dropped, while all other quoted cuts on the D* and the muon remained unchanged. To obtain a clean DIS sample, the following additional cuts were applied: a reconstructed electron with E>10 GeV satisfying some quality cuts, $Q^2 > 2$ GeV^2, and inelasticity $0.05 < y < 0.7$ (same DIS cuts as used in the ZEUS high pt muon + jet analysis [4]). The resulting D^* mass peaks for the like and unlike $D^* - \mu$ charge combinations are shown in Fig. 1.

The number of background events under the D^* mass peaks (fake D^*) was estimated using the wrong-sign $K\pi$ combinations. Dedicated studies revealed that the bias induced by charge correlations is minimized by disregarding the charge relationship between the muon and D^* for this estimate of the background. The wrong-charge $K\pi$ contributions obtained in this way were normalised to the data outside the D^* peak, separately for the like-sign and unlike-sign $\mu - D^*$ sample, as shown in Fig. 1.

Monte Carlo (MC) simulations of beauty and charm production were performed using the PYTHIA [8], RAPGAP [9] and HERWIG [10] generators. These simulations include the direct photon-gluon-fusion process, flavour excitation in the resolved photon and proton, and the QCD-Compton process. Gluon splitting into heavy flavours in the initial or final

states of light-quark events was not included in the simulation; this contribution is, however, expected to be small. The detector simulation includes the simulation of both real and fake muons (in addition to a real D^* from charm or beauty). Background containing both a fake muon and a fake D* is included in the fake-D^* background estimated directly from the data. It does therefore not need to be simulated.

Fake muons can be produced by hadron showers leaking from the back of the calorimeter or by charged hadrons traversing the entire calorimeter without interaction. In addition, low-momentum muons can come from in-flight decays of pions and kaons. Finally, tracks reconstructed in the central tracker may be wrongly associated to a signal from a real muon in the muon chambers. A dedicated study based on pions from K^0 decays showed that the detector simulation reproduced these backgrounds reasonably well.

4 Signal extraction

In the following, the signal extraction procedure is described for the inclusive sample. The dedicated DIS sample, which has significantly less statistics, is treated in an analogous way.

Figure 2 shows the distribution of the angular difference $\Delta R = \sqrt{\Delta\phi^2 + \Delta\eta^2}$ between the D^* and the muon and the mass of the $\mu - D^*$ system for events passing all event selections, including the ΔM cut. The distributions are shown for like- and unlike-sign $\mu - D^*$ events separately. The expected signal and background contributions, normalised to the fractions determined later in the analysis, are also indicated. For unlike-sign events, the region $\Delta R > 2$, which predominantly correponds to the back-to-back configuration, is clearly dominated by events from charm. In contrast, the region $\Delta R < 2$ is enriched in beauty events, in which the D^* and muon originate mainly from decays of the same parent B hadron. This is illustrated further in the $\mu - D^*$ invariant mass distribution (Fig. 2) for events in the beauty-enriched region ($\Delta R < 2$). A peak which can be attributed to the partial reconstruction of the decaying B meson is clearly visible. A comparison with the like-sign sample shows that the low-mass edge of this peak is dominated by background. An invariant-mass cut of 3 GeV $< M(\mu - D^*) <$ 5 GeV was therefore applied to the $\Delta R < 2$ subsample.

The ΔR and $\Delta\phi$ distributions, after this additional cut and after subtraction of the fake D^* background, are shown in Fig. 3 together with a fit of the relative contributions from charm and beauty. The fake-muon background (from charm) was fixed to the relative fraction predicted by the MC simulation. The variation of this contribution within the limits allowed by the like-sign sample (which is dominated by this background) is part of

the systematic uncertainty quoted below. The result for the fraction of beauty events in the final inclusive sample shown in Fig. 3, using the shapes predicted by PYTHIA, is:

- $f_b = 0.363 \pm 0.084$(stat.) for the ΔR and
- $f_b = 0.348 \pm 0.080$(stat.) for the $\Delta\phi$ distribution.

The ΔR result was chosen as the reference, and the $\Delta\phi$ result used as a systematic check. With these fitted fractions, the $\Delta M(D^* - D^0)$ distributions are shown separately for $\Delta R < 2$ and $\Delta R > 2$ in Fig. 4. The corresponding number of beauty, charm, and fake-muon candidates is indicated in each case. In the unlike-sign part, the beauty and charm contributions are now separated, with only small cross-contaminations. Agreement is seen, even in the like-sign part, which was not included in the fit.

The analogous results for the DIS sample are shown in Figs. 5 and 6. The fitted beauty fractions, using the shapes predicted by RAPGAP, are

- $f_b = 0.51 \pm 0.25$(stat.) for the ΔR and
- $f_b = 0.45 \pm 0.33$(stat.) for the m(D$^*\mu$) distribution.

The $\Delta\phi$ fit was not used here since, although consistent, it did not yield a significant result. Again, the ΔR result is chosen as the reference, and the other as a cross check.

5 Results

The measured beauty fraction in the inclusive samnple was used to estimate the cross section for the process $ep \to eb\bar{b}X \to eD^*\mu X$ in the kinematic range $p_T^{D^*} > 1.9$ GeV, $-1.5 < \eta^{D^*} < 1.5$, $p_T^{\mu} > 1.4$ GeV and $-1.75 < \eta^{\mu} < 1.3$ as:

$$\sigma(ep \to eb\bar{b}X \to eD^*\mu X) = 214 \pm 52(\text{stat.})^{+96}_{-84}(\text{syst.})\ \text{pb}.$$

After adjusting the values for differences in the selected kinematic range, this result is in good agreement with a similar measurement [11] by the H1 collaboration.

The largest contributions to the systematic uncertainty arise from varying the shape of the muon and D^* p_T spectra used for the acceptance calculation and from the differences in fragmentation and the $b\bar{b}$ correlations (including parton showering) predicted by HERWIG and PYTHIA. The detection efficiency was corrected for residual differences in the reconstruction and trigger efficiencies in data and MC. The cross sections predicted by PYTHIA and HERWIG in the same kinematic regime are significantly lower, $\sigma(ep \to eb\bar{b}X \to eD^*\mu X) = 80$ and 38 pb, respectively.

In order to compare the measured cross section with next-to-leading-order (NLO) QCD predictions for beauty production, the visible cross section needs to be extrapolated to a

cross section at the b-quark level. Since NLO predictions only exist separately for the DIS and photoproduction regimes, cross sections have also been determined separately for the two cases.

A photoproduction subsample was selected from the inclusive sample by removing events with a clear DIS electron (positron) candidate and by requiring the inelasticity y to satisfy $y < 0.85$. After repeating the above fitting and cross section extraction procedure a visible cross section in the kinematic range $Q^2 < 1$ GeV^2 and $0.05 < y < 0.85$ was obtained:

$$\sigma_{PHP}(ep \to eb\bar{b}X \to eD^*\mu X) = 159 \pm 41(\text{stat.})^{+68}_{-62}(\text{syst.}) \text{ pb}.$$

A DIS subsample was selected by requiring an identified DIS electron, and the number of events was increased by loosening some of the cuts on the D*, as described in Section 3 for the dedicated DIS selection. From the fitted beauty fraction (section 4), a visible cross section in the kinematic range $Q^2 > 2$ GeV^2, $0.05 < y < 0.7$ and $p_T^{D^*} > 1.5$ GeV (other D^* and muon cuts same as above) was obtained:

$$\sigma_{DIS}(ep \to eb\bar{b}X \to eD^*\mu X) = 60 \pm 29(\text{stat.})^{+30}_{-23}(\text{syst.}) \text{ pb}.$$

Again, the cross sections predicted from RAPGAP (used for the central signal extraction) and HERWIG (used for systematic checks, in particular for differences in the b$\bar{\text{b}}$ correlations) in the same kinematic regime are considerably lower, $\sigma(ep \to eb\bar{b}X \to eD^*\mu X) =$ 26 and 10 pb, respectively.

As the D^* and muon in the beauty-enriched region are generally produced from the same b quark, the b-level cross section is quoted for individual b or $\bar{b}$ production rather than for correlated $b\bar{b}$ pair production. A significant fraction of the parent b quarks of the selected events is expected to have very low p_T^b values. Therefore, a cross section with no cut on p_T^b has been measured. Furthermore, there is a strong correlation between the pseudorapidity of the $\mu - D^*$ system and the longitudinal rapidity of the parent b quark. In order to reflect the limited angular acceptance of the detector for both the D^* and the muon, the cross-section measurement was restricted to the b-quark rapidity range $\zeta^b < 1$. In this range, restricted to photoproduction, the p_T^b and ζ^b distributions of PYTHIA (after parton showering) agree with the central NLO b-quark spectra from Frixione et al. (FMNR) [12] to within $\pm 15\%$. Therefore, PYTHIA was used to extrapolate the visible cross section for the photoproduction region. Similarly, the corresponding RAPGAP spectra for the DIS case agree with the central NLO predictions from Harris and Smith (HVQDIS) [13, 14].

Part of the systematic uncertainty of the visible cross section is related to the extrapolation of the beauty contribution measured at low ΔR into the high ΔR region (see Fig. 3), which depends on the details of the implementation of $b\bar{b}$ correlations. A large part of this systematic uncertainty cancels in the extrapolation to a single b- or $\bar{b}$-quark cross section.

On the other hand, the extrapolation implies additional systematic uncertainties from the b-quark fragmentation and decay and the details of the shape of the p_T^b spectrum. The result for the extrapolated cross section for $\zeta^b < 1,\ Q^2 < 1\ \mathrm{GeV}^2,\ 0.05 < y < 0.85$ and $m_b = 4.75$ GeV is:

$$\sigma(\gamma^* p \to b(\bar{b})X)_{PHP} = 15.1 \pm 3.9(\mathrm{stat.})\ ^{+3.8}_{-4.7}(\mathrm{syst.})\ \mathrm{nb}.$$

The corresponding result for the extrapolated cross section for $\zeta^b < 1,\ Q^2 > 2\,\mathrm{GeV}^2,\ 0.05 < y < 0.7$ and $m_b = 4.75$ GeV is:

$$\sigma(\gamma^* p \to b(\bar{b})X)_{DIS} = 3.2 \pm 1.5(\mathrm{stat.})\ ^{+0.9}_{-1.0}(\mathrm{syst.})\ \mathrm{nb}.$$

In addition to the errors propagated from the visible cross section, the systematic uncertainty includes the errors on b-quark fragmentation and the branching ratios obtained from a comparison of the PYTHIA/RAPGAP and HERWIG acceptances, and assumes the validity of the NLO p_T^b shape used for the extrapolation. This is to be compared to the NLO prediction for the same kinematic range using the FMNR calculation [12] of

$$\sigma_{NLO}(\gamma^* p \to b(\bar{b})X)_{PHP} = 5.0^{+1.7}_{-1.1}\ \mathrm{nb}$$

for $\mu_R = \mu_F = \mu_0 = \sqrt{m_b^2 + p_T^{b2}}$ and $m_b = 4.75$ GeV, where μ_R and μ_F are the renormalisation and factorisation scales, respectively. The errors were calculated by simultaneously varying the above parameters in the range $\mu_0/2 < \mu < 2\mu_0$ and $4.5 < m_b < 5$ GeV.

The corresponding NLO HVQDIS [13, 14] prediction is

$$\sigma_{NLO}(\gamma^* p \to b(\bar{b})X)_{DIS} = 0.87^{+0.28}_{-0.16}\ \mathrm{nb}$$

for $\mu_R = \mu_F = \mu_0 = \sqrt{m_b^2 + Q^2}$ and $m_b = 4.75$ GeV, with the same variation of scales and m_b.

These cross sections are presented in Fig. 7.

6 Conclusions

The cross section for beauty production in ep collisions at HERA has been measured using an analysis technique based on the detection of a muon and D^* from a b and/or $\bar{b}$ decay. The resulting visible cross sections significantly exceed leading-order plus parton-shower MC expectations. Since the analysis is sensitive to b-quark production near the kinematic threshold, the visible cross sections were extrapolated to b-quark production cross sections in photoproduction and DIS without an explicit cut on p_T^b. These cross sections were compared to NLO QCD predictions.

References

[1] H1 Coll., C. Adloff et al., Phys. Lett. **B 467**, 156 (1999);
ZEUS Coll., J. Breitweg et al., Eur. Phys. J. **C 18**, 625 (2001).

[2] H1 Coll. H1prelim-03-072, Abstract 5-0164, International Europhysics Conference on High Energy Physics, Aachen, Germany, July 17-23, 2003;
H1 Coll. H1prelim-04-071, presented at DIS2004, Strbske Pleso, Slovakia, April 14-18, 2004.

[3] ZEUS Coll., S. Chekanov et al. (2003). hep-ex/0312057, accepted by Phys. Rev. D.

[4] ZEUS Coll., S. Chekanov et al. (2004). hep-ex/0405069, submitted to Phys. Lett. B.

[5] ZEUS Coll. Abstract 784, International Conference on High Energy Physics, Amsterdam, The Netherlands, July 24-31, 2002.

[6] ZEUS Coll., U. Holm (ed.), *The ZEUS Detector*. Status Report (unpublished), DESY (1993), available on `http://www-zeus.desy.de/bluebook/bluebook.html`.

[7] N. Harnew et al., Nucl. Inst. Meth. **A 279**, 290 (1989);
B. Foster et al., Nucl. Phys. Proc. Suppl. **B 32**, 181 (1993);
B. Foster et al., Nucl. Inst. Meth. **A 338**, 254 (1994).

[8] T. Sjöstrand, Comp. Phys. Comm. **82**, 74 (1994).

[9] H. Jung, Comp. Phys. Comm. **86**, 147 (1995).

[10] G. Marchesini et al., Comp. Phys. Comm. **67**, 465 (1992).

[11] J. Wagner, H1 Coll. H1prelim-02-071, talk presented at DIS2002, Cracow, Poland, April 30 - May 4, 2002.

[12] S. Frixione, P. Nason and G. Ridolfi, Nucl. Phys. **B 454**, 3 (1995).

[13] B.W. Harris and J. Smith, Nucl. Phys. **B452**, 109 (1995).

[14] B.W. Harris and J. Smith, Phys. Lett. **B353**, 535 (1995).

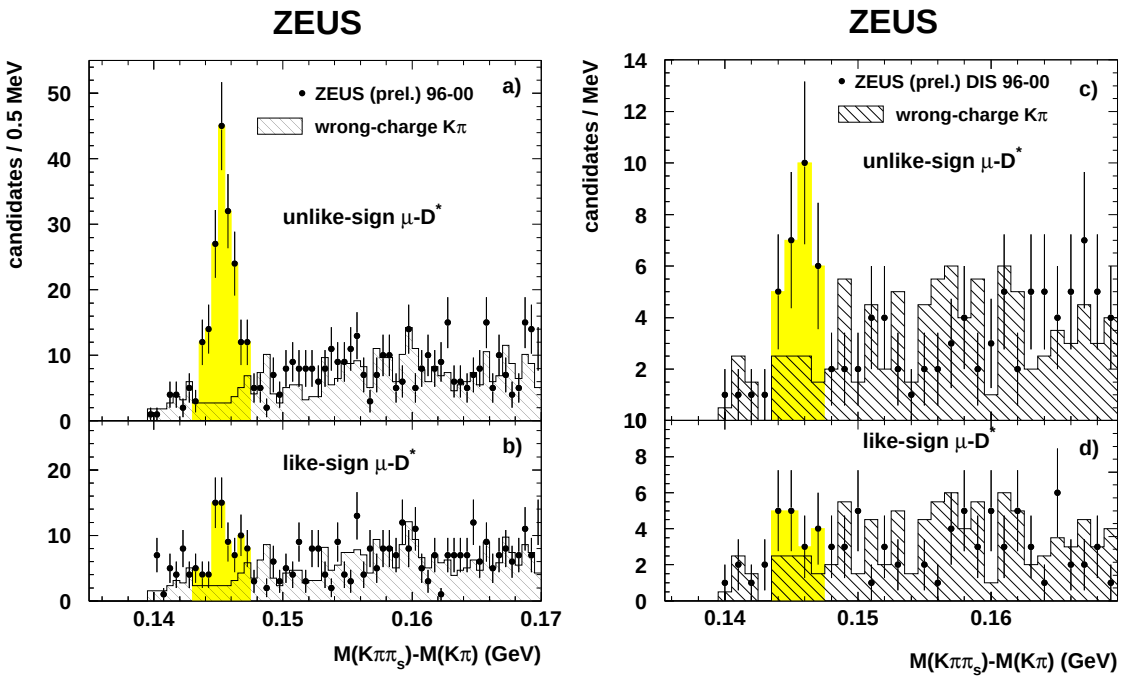

Figure 1: *Distribution of $\Delta M(D^* - D^0)$ for data (full circles), and combinatorial background (hatched histogram) for a) inclusive unlike-sign b) inclusive like-sign c) DIS unlike-sign and d) DIS like-sign muon-D^* combinations. The D^* signal region is indicated by the shaded area.*

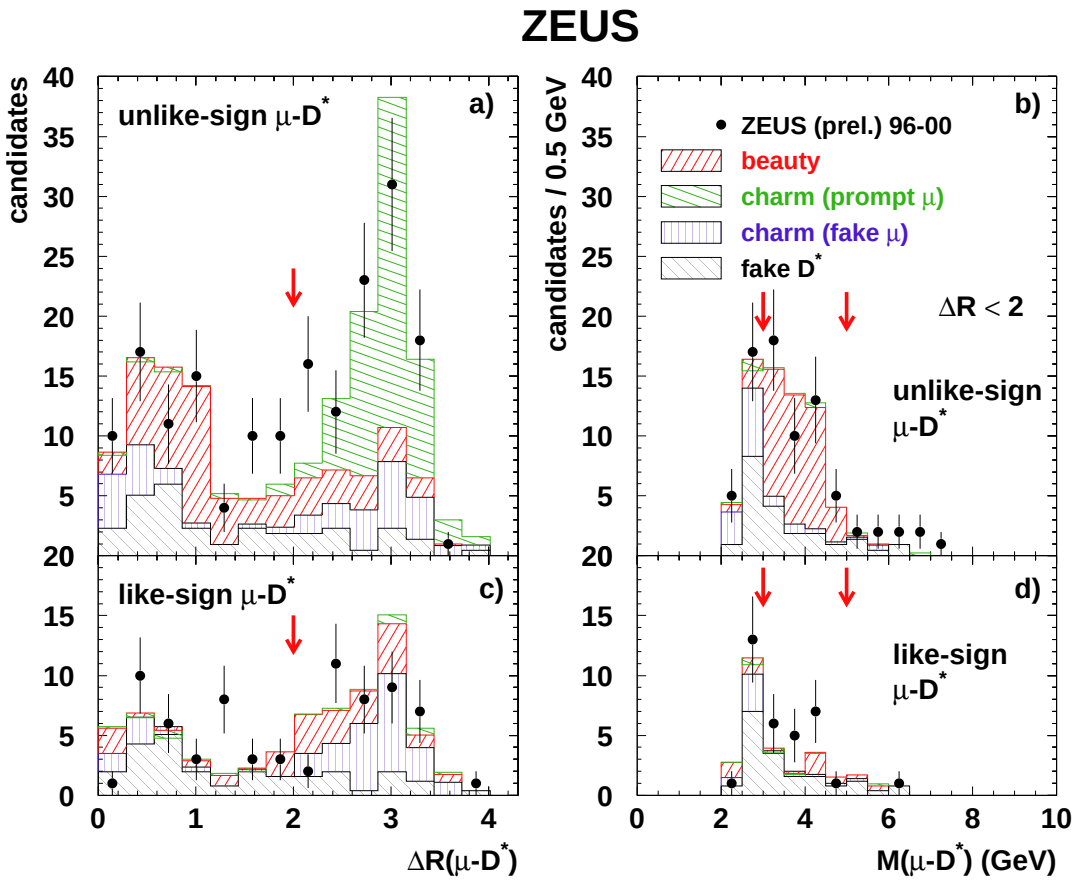

Figure 2: *a,c) Distribution of $\Delta R(\mu - D^*)$ and b,d) $M(\mu - D^*)$ for inclusive data (full circles), beauty and charm signal, and fake-μ and fake-D^* backgrounds. The latter are distinguished by different hatch styles. Unlike-sign and like-sign $\mu - D^*$ combinations are shown separately. Cuts described in the text are indicated by the arrows.*

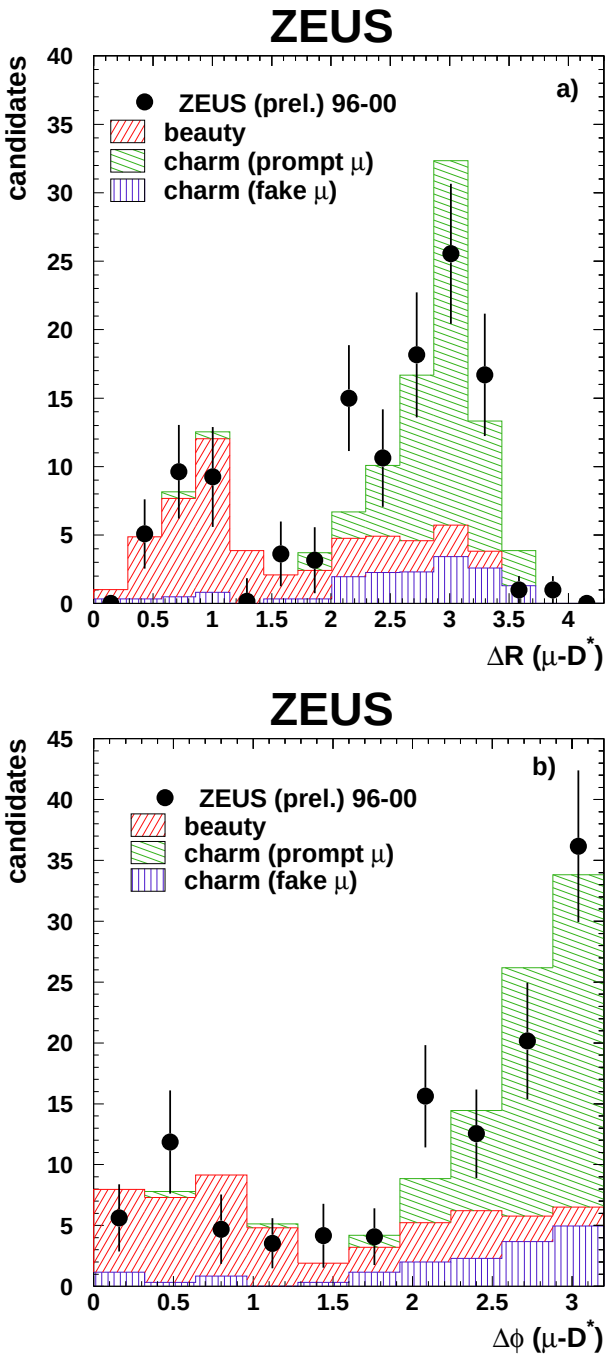

Figure 3: *a) ΔR and b) $\Delta\phi$ distributions of the D^*-muon system for inclusive unlike-sign events, after subtraction of the fake-D^* background. Data points (full circles) are shown together with the fitted contributions from beauty and charm, as indicated in the legend. The fake-muon contribution from charm is shown separately, but fitted together with the charm contribution. The beauty contribution includes a very small fraction of fake muons from beauty.*

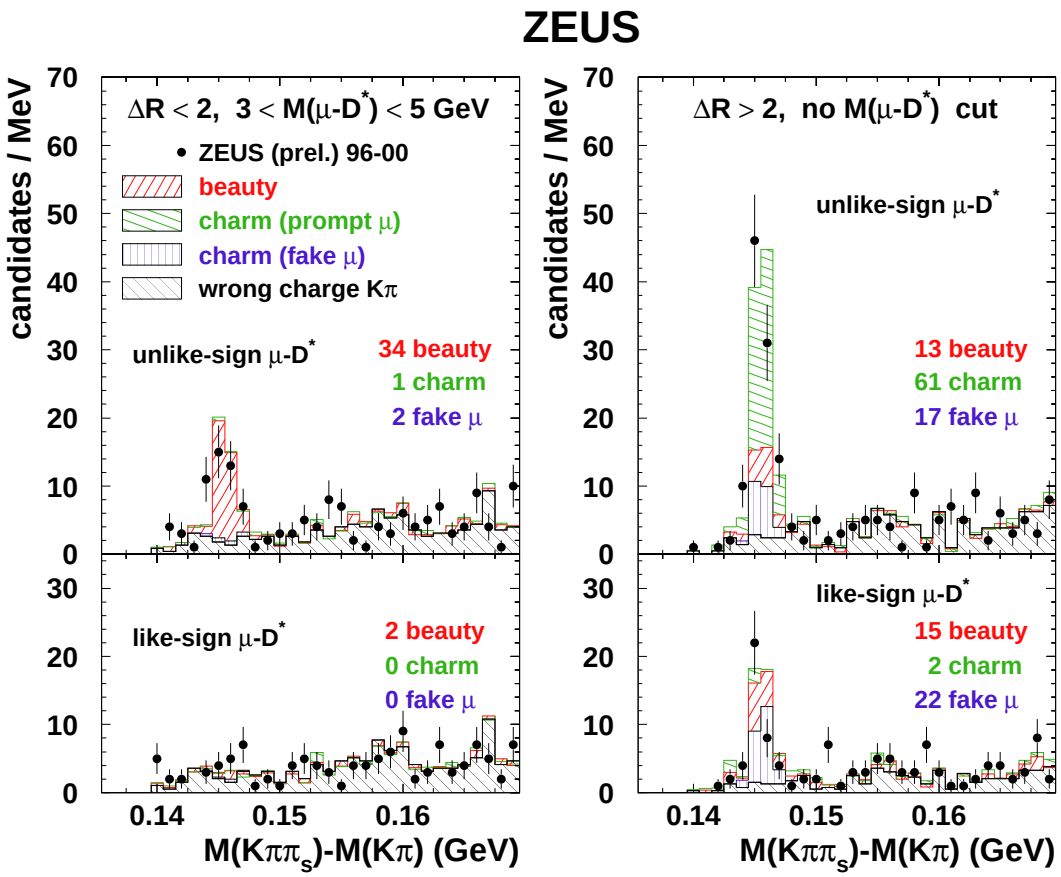

Figure 4: *$\Delta M(D^* - D^0)$ distributions for four different regions of inclusive phase space. The data are shown as full circles. The beauty and charm contributions, and the fake muon and combinatorial D^* backgrounds are indicated as shown in the legend. The number (rounded to the nearest integer) of beauty, charm and fake-muon candidates is indicated in each figure.*

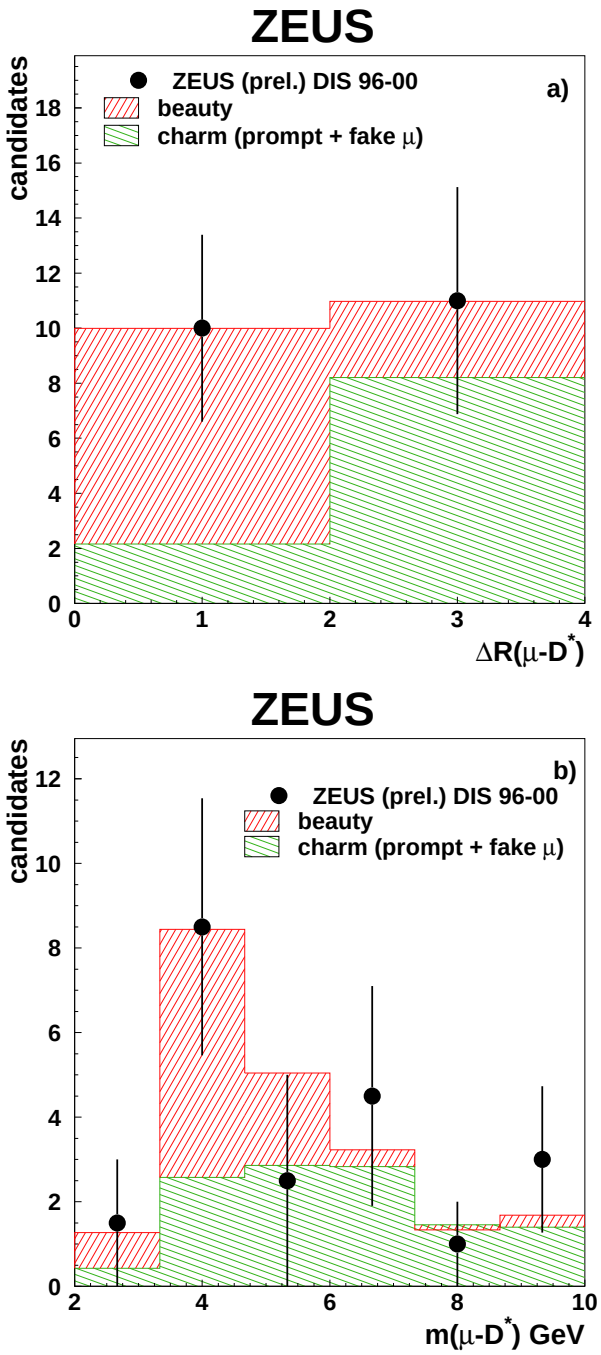

Figure 5: *a) ΔR and b) $m(D^*/mu)$ distributions of the D^*-muon system for DIS unlike-sign events, after subtraction of the fake-D^* background. Data points (full circles) are shown together with the fitted contributions from beauty and charm, as indicated in the legend. The fake-muon contribution from charm is included in the charm contribution. Its fraction is similar to the one in Fig. 3. The beauty contribution includes a very small fraction of fake muons from beauty.*

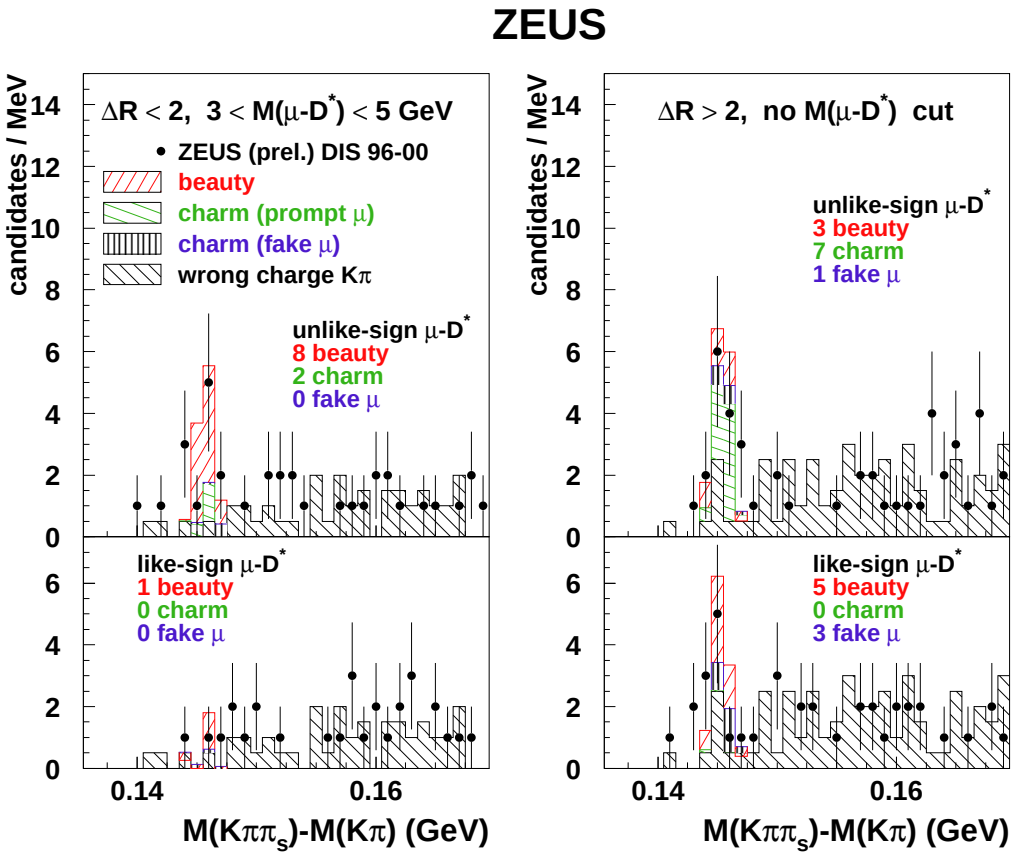

Figure 6: *$\Delta M(D^* - D^0)$ distributions for four different regions of DIS phase space. The data are shown as full circles. The beauty and charm contributions, and the fake muon and combinatorial D^* backgrounds are indicated as shown in the legend. The number (rounded to the nearest integer) of beauty, charm and fake-muon candidates is indicated in each figure.*

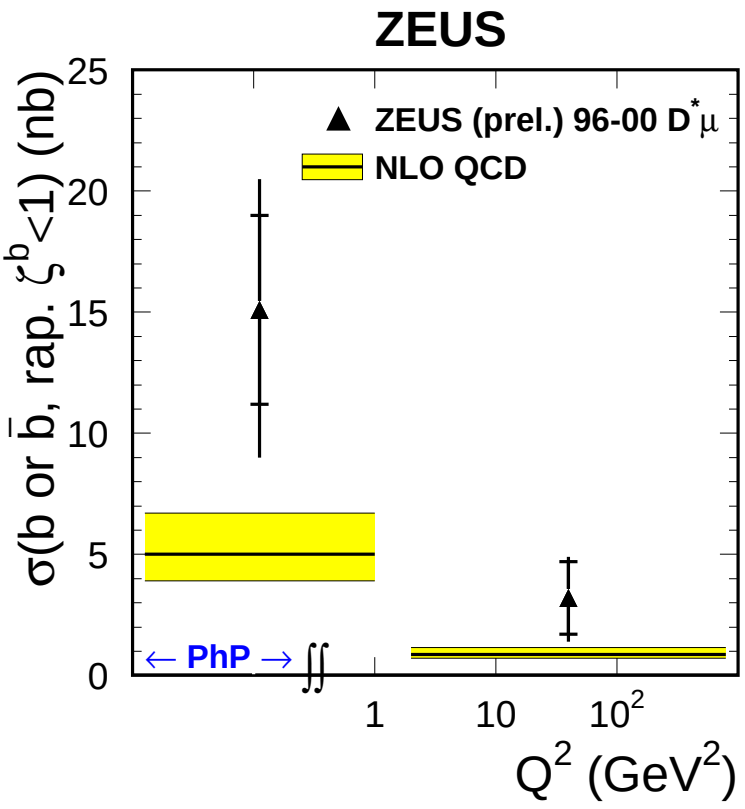

Figure 7: *Cross section for single b or $\bar{b}$-quark production in the rapidity range $\zeta^b < 1$ for photoproduction (PHP, left) and DIS (right), compared to NLO QCD predictions from FMNR (left) and HVQDIS (right). The PHP cross section is for $0.05 < y < 0.85$, and the DIS cross section for $0.05 < y < 0.7$. The cross sections are integrated over the indicated Q^2 ranges, and over the full p_T^b range. More details on the QCD calculations are given in the text.*